

Co-AttenDWG: Co-Attentive Dimension-Wise Gating and Expert Fusion for Multi-Modal Offensive Content Detection

Md. Mithun Hossain[✉], Md. Shakil Hossain[✉], Sudipto Chaki[✉], M. F. Mridha[✉], *Senior Member, IEEE*

Abstract—Multi-modal learning has become a critical research area because integrating text and image data can significantly improve performance in tasks such as classification, retrieval, and scene understanding. However, despite progress with pre-trained models, current approaches are limited by inadequate cross-modal interactions and static fusion strategies that do not fully exploit the complementary nature of different modalities. To address these shortcomings, we introduce a novel multi-modal Co-AttenDWG architecture that leverages dual-path encoding, co-attention with dimension-wise gating, and advanced expert fusion. Our approach begins by projecting text and image features into a common embedding space, where a dedicated co-attention mechanism enables simultaneous, fine-grained interactions between modalities. This mechanism is further enhanced by a dimension-wise gating network that adaptively regulates the feature contributions at the channel level, ensuring that only the most relevant information is emphasized. In parallel, dual-path encoders refine the representations by processing cross-modal information separately before an additional cross-attention layer further aligns modalities. The refined features are then aggregated via an expert fusion module that combines learned gating and self-attention to produce a robust, unified representation. We validate our approach on the MIMIC and SemEval Memotion 1.0, where experimental results demonstrate significant improvements in cross-modal alignment and state-of-the-art performance, underscoring the potential of our model for a wide range of multi-modal applications.

Impact Statement—The Co-AttenDWG architecture redefines multi-modal learning by overcoming limitations inherent in static fusion techniques. Integrating dual-path encoding, co-attention with dimension-wise gating, and advanced expert fusion, it dynamically harnesses complementary textual and visual cues in a unified embedding space. This approach significantly enhances cross-modal alignment and performance, as evidenced by state-of-the-art results on the MIMIC and SemEval Memotion datasets. By adaptively modulating feature contributions and refining representations, Co-AttenDWG not only boosts detection accuracy but also opens new avenues for intelligent, context-aware systems across domains such as content analysis, sentiment evaluation, and complex scene

Md. Mithun Hossain, Md. Shakil Hossain, and Sudipto Chaki are with the Department of Computer Science and Engineering, Bangladesh University of Business and Technology, Dhaka 1216, Bangladesh; e-mail: (mhosen751@gmail.com, shakilhosen3.1416@gmail.com, sudiptochakibd@gmail.com).

M. F. Mridha is with the Department of Computer Science, American International University-Bangladesh, Dhaka 1229, Bangladesh (email: firoz.mridha@aiub.edu).

Corresponding Author: M. F. Mridha (e-mail: firoz.mridha@aiub.edu)
Manuscript received Month xx, 20xx; revised Month xx, 20xx.

understanding. This breakthrough paves the way forward.

Index Terms—Co-AttenDWG, Cross-Attention, Mixture-of-Experts, Offensive Content Detection, Multi-modal Learning.

I. INTRODUCTION

MULTI-modal learning has emerged as a transformative paradigm in artificial intelligence, driven by the need to integrate diverse data sources such as text, images, audio, and video to provide a holistic understanding of complex real-world scenarios [1]–[3]. This integration is particularly important in tasks such as classification, sentiment analysis, and information retrieval, where combining complementary modalities can reveal patterns and insights that remain hidden when each modality is independently processed [4]. Traditional methods typically processes each modality separately and then merges the results using simple concatenation or fixed-weight averaging techniques [2], but these basic fusion approaches often fail to capture the intricate interdependencies and correlations among modalities, resulting in representations that do not fully utilize the available information and consequently, limit the overall model performance [5].



(a) Meme illustrating textual and visual interplay. (b) Another meme combining images and text.

Fig. 1: Examples of memes that combine textual cues with visual context, illustrating the challenges of multi-modal integration. Both examples demand nuanced interpretation of text, facial expressions, and background details.

Figure 1 clearly illustrates the challenges inherent in multi-modal data: the first image (Figure 1a) demonstrates the complex interplay between textual cues and visual context, while the second image (Figure 1b) emphasizes the subtle visual nuances and layered textual information that must be interpreted accurately. These examples highlight the inherent difficulties faced by traditional fusion methods, which often rely on static, simplistic approaches that fail to capture the dynamic, context-dependent relationships between modalities. In response to this problem, researchers have turned to advanced pre-trained

models to overcome these limitations. Models such as BERT have significantly advanced natural language processing [6], and convolutional neural networks have transformed computer vision [7], [8]. Although these models excel at extracting robust modality-specific features, integrating these powerful representations into a unified multi-modal framework remains challenging. Current fusion strategies often struggle to align and combine the complementary features effectively, underscoring the need for more adaptive, context-aware mechanisms such as those proposed in our Co-AttenDWG architecture to fully leverage the potential of multi-modal learning [9].

To address these limitations, we propose a novel multi-modal **Co-AttenDWG** architecture that integrates dual-path encoding, co-attention with dimension-wise gating, and advanced expert fusion into a unified framework. Our model begins by projecting features from both modalities into a common embedding space, setting the stage for deep interaction. A dedicated co-attention mechanism then facilitates simultaneous, fine-grained cross-modal interactions. By incorporating a dimension-wise gating network, **Co-AttenDWG** dynamically modulates feature contributions at the channel level, ensuring that the most informative aspects of each modality are selectively emphasized during the fusion process. We validate our approach on challenging datasets such as MIMIC and SemEval Memotion 1.0, which demand robust multi-modal understanding. Experimental results reveal that our architecture significantly improves cross-modal alignment and outperforms state-of-the-art methods, demonstrating its potential to advance the field of multi-modal learning. This work not only addresses the current limitations of static fusion strategies but also opens avenues for more adaptive and context-aware integration of heterogeneous data sources in future research.

The key contributions of this work are summarized as follows:

- We design a novel multi-modal **Co-AttenDWG** architecture that processes text and image features in a dual-path encoding framework, enabling robust alignment and refined representations.
- We introduce a co-attention mechanism with dimension-wise gating that dynamically modulates channel-level feature contributions, enhancing fine-grained cross-modal interactions.
- We develop an advanced expert fusion module that integrates learned gating with additional self-attention, effectively combining modality-specific representations into a unified embedding.

The rest of this paper is organized as follows. [Section II](#) discusses related work in multi-modal offensive content detection and cross-modal fusion techniques. [Section III](#) outlines the **Co-AttenDWG** framework, including its key components and architectural design. [Section IV](#) presents our experiment, results, and provides a detailed analysis. Finally, [Section V](#) concludes the paper and highlights future research directions.

II. LITERATURE

Recent advances in multi-modal offensive content detection have increasingly focused on uniting textual and visual cues

to improve performance beyond traditional unimodal systems. Early studies demonstrated that integrating features from pre-trained language models and computer vision architectures can significantly enhance detection accuracy. For example, Rana and Jha [10] introduced a multimodal framework that fused BERT/ALBERT-based text analysis with acoustic emotion cues in short videos, resulting in a notable reduction of false positives, particularly in discerning sarcasm from genuine hate speech. Likewise, Birhane et al. [11] critically assessed large-scale multimodal dataset revealing challenges related to explicit bias and noise while Suryawanshi et al. [12] showed that early fusion of text and image features in meme analysis yields improved detection results. In contrast, unimodal approaches [13]–[15] that process either text or image data in isolation have consistently underperformed compared to models leveraging cross-modal interactions, underscoring the necessity for more integrated methods.

Efficiently merging heterogeneous signals from different modalities is key to unlocking the full potential of multi-modal systems [16]. A variety of fusion strategies have been explored in the literature. Discriminative joint multi-task frameworks, such as the one proposed by Zheng et al. [17], utilize both intra- and inter-task dynamics to enhance sentiment prediction. Chen et al. [18] further demonstrated that jointly fusing textual and visual features significantly improves classification accuracy by exploiting the complementary information inherent to each modality. While early and late fusion techniques [19], [20] offer a straightforward means for feature integration, they often suffer from modality-specific information loss or misalignment. Hybrid approaches, which blend the strengths of both strategies [21]–[24] have provided more robust alternatives. Moreover, the introduction of cross-attention mechanisms has allowed for fine-grained interactions between visual and textual embeddings, as evidenced by recent studies from Mao et al. [25] and Li et al. [26]. Graph-based fusion approaches [27], [28] have also emerged, enabling models to capture contextual relationships through structured representations and addressing some limitations of simple concatenation schemes.

Although pre-trained models have advanced feature extraction from both text and image domains, current multi-modal offensive content detection systems still rely on static fusion technique such as simple concatenation that inadequately capture the dynamic, context-dependent interplay between modalities. Existing attention-based methods improve cross-modal alignment, yet they often neglect adaptive channel-wise gating and expert-based fusion, limiting interpretability and robustness, particularly under noisy or ambiguous conditions. Models that rely solely on such static fusion techniques often fail to capture dynamic, structured cross-modal interactions in a bidirectional manner [17]. Furthermore, recent studies indicate that incorporating adaptive gating and expert fusion mechanisms substantially enhances a model's ability to integrate complementary cues, resulting in improved performance and explainability [18]. To address these gaps, our proposed Co-AttenDWG model (see [Figure 2](#)) projects text and image features into a shared space and employs bidirectional co-attention coupled with a dimension-wise gating mechanism

to emphasize salient cues. An advanced expert fusion module then adaptively combines modality-specific representations to enhance interpretability and performance, as further validated in our case studies. This dynamic, context-aware framework effectively overcomes the limitations of current static fusion strategies.

III. PROPOSED METHODOLOGY

Figure 2 presents our proposed architecture, **Co-AttenDWG**, which addresses the challenges of multi-modal offensive content detection. Offensive content detection in multi-modal settings is challenging because text $X_{\text{text}} \in \mathbb{R}^{B \times L}$ and images $X_{\text{img}} \in \mathbb{R}^{B \times H \times W \times C}$ are processed through distinct pipelines that produce heterogeneous feature representations. For example, text is encoded using a model such as BERT [6] that generates hidden states $H \in \mathbb{R}^{B \times L \times D_{\text{text}}}$ and extracts the representative [CLS] token $h_{\text{CLS}} = H[:, 0, :] \in \mathbb{R}^{B \times D_{\text{text}}}$, which is then projected into a common embedding space to obtain $T \in \mathbb{R}^{B \times D}$. Similarly, image features are extracted from a CNN such as VGG16 [7] to produce a feature vector $f \in \mathbb{R}^{B \times D_{\text{img}}}$, which is also projected into the same space as $I \in \mathbb{R}^{B \times D}$. Traditional fusion strategies, such as simple concatenation $F = [T; I]$, do not capture the dynamic, context-dependent cross-modal interactions needed for robust detection. To overcome these limitations, our method defines an adaptive fusion function $\mathcal{F}(T, I)$ that produces a unified feature representation $E \in \mathbb{R}^{B \times D}$ by aligning heterogeneous modalities. This figure illustrates how our approach, through bidirectional fusion with co-attentive dimension-wise gating and expert fusion, emphasizes the most relevant features from each modality to enhance detection performance.

A. Multi-Modal Feature Extraction and Projection

In the text branch, we tokenize the input and process it with a pre-trained model such as BERT [6] to obtain a sequence of hidden states, from which we extract the [CLS] token as an overall semantic summary. This token is then projected into a common D -dimensional embedding space using a learned linear transformation and reshaped into a sequence for later integration. In the image branch, each image is passed through a CNN like VGG16 [7] to extract high-level visual features, which are subsequently projected into the same D -dimensional space and reshaped into a sequence. Aligning both modalities in this shared embedding space reduces heterogeneity and lays a robust foundation for subsequent fusion processes that effectively combine complementary information for improved offensive content detection.

B. Bidirectional Fusion with Co-Attentive Dimension-Wise Gating

We design a bidirectional fusion module to integrate features from text and image modalities while capturing fine-grained cross-modal interactions. Our approach first applies cross-modal attention [9] and then refines the outputs using a dimension-wise gating mechanism [29].

Cross-Modal Co-Attention: We let the text modality attend to the image modality by computing multi-head attention. Specifically, we use the text feature sequence $T_{\text{seq}} \in \mathbb{R}^{B \times 1 \times D}$ as the query and the image feature sequence $I_{\text{seq}} \in \mathbb{R}^{B \times 1 \times D}$ as both key and value. This yields:

$$A_{t \rightarrow i} = \text{MHA}(Q = T_{\text{seq}}, K = I_{\text{seq}}, V = I_{\text{seq}}) \in \mathbb{R}^{B \times 1 \times D}, \quad (1)$$

which captures the image-informed features for the text modality. Similarly, we allow the image modality to attend to the text modality by using I_{seq} as the query and T_{seq} as both key and value:

$$A_{i \rightarrow t} = \text{MHA}(Q = I_{\text{seq}}, K = T_{\text{seq}}, V = T_{\text{seq}}) \in \mathbb{R}^{B \times 1 \times D}. \quad (2)$$

Dimension-Wise Gating: After obtaining the attention outputs, we refine them using a channel-wise gating mechanism. For the text branch, we compute a gating weight:

$$G_t = \sigma(W_{g,t} A_{t \rightarrow i} + b_{g,t}) \in \mathbb{R}^{B \times 1 \times D}, \quad (3)$$

where σ is the sigmoid activation. This weight is then applied element-wise to the text attention output to obtain the gated text feature:

$$\tilde{T} = G_t \odot A_{t \rightarrow i}, \quad (4)$$

as shown in Equation (4). Similarly, for the image branch, we compute:

$$G_i = \sigma(W_{g,i} A_{i \rightarrow t} + b_{g,i}) \in \mathbb{R}^{B \times 1 \times D}, \quad (5)$$

and derive the gated image feature:

$$\tilde{I} = G_i \odot A_{i \rightarrow t}. \quad (6)$$

These steps align and enhance the features by emphasizing the most relevant information in each channel. The bidirectional attention, as defined in Equations (1) and (2), allows the modalities to inform each other, while the dimension-wise gating (Equations (3)–(6)) selectively filters the features. This process improves the robustness of the subsequent fusion mechanism, enabling the model to dynamically capture cross-modal interactions and adaptively weight the contributions of each modality for more effective offensive content detection.

C. Dual-Path Encoding and Cross-Attention

After refining the features with bidirectional co-attention and dimension-wise gating, we further enhance the representations through dual-path encoding and additional cross-attention mechanisms to refine and align the modalities before fusion.

Dual-Path Encoding: The gated features are processed via MambaFormer-based encoder modules that combine self-attention and convolutional operations to capture both local and global context [9], [29]. For the text modality, we feed the gated image feature $\tilde{I} \in \mathbb{R}^{B \times 1 \times D}$ into the text-to-image MambaFormer encoder to obtain a refined representation:

$$Z_{t \rightarrow i} = \text{MambaFormerEncoder}(\tilde{I}) \in \mathbb{R}^{B \times 1 \times D}, \quad (7)$$

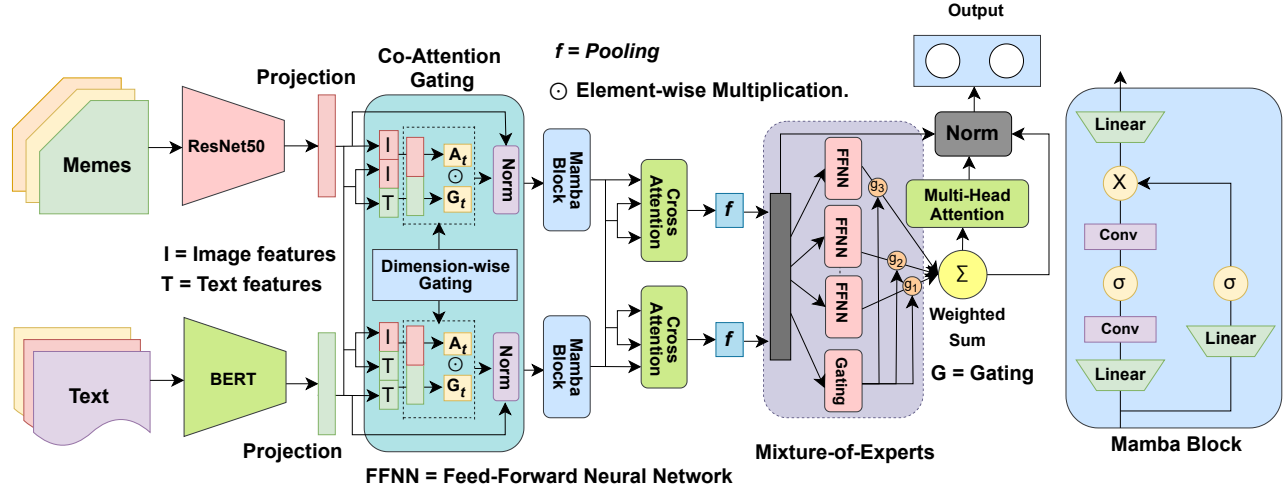


Fig. 2: A high-level overview of our Co-AttenDWG architecture for multi-modal offensive content detection. The image branch (top) processes memes through a pre-trained CNN (VGG16), extracting high-level visual features I . Meanwhile, the text branch (bottom) encodes input sentences using a language model such as DistilBERT, yielding textual features T . Both sets of features are projected into a shared embedding space and enter the co-attention gating block, where dimension-wise gating adaptively emphasizes salient channels from each modality. The attention outputs, highlighted as A_i for images and A_t for text, pass into a mixture-of-experts fusion mechanism that combines relevant cross-modal cues. Next, the fused representation flows through the Mamba block, which integrates local convolutional operations and multi-head self-attention to refine context. Finally, the aggregated features are projected via linear layers to produce the final output, representing the predicted offensive content class. This design promotes dynamic cross-modal interactions and expert gating, enabling effective offensive content detection in both text and images.

which is then fused with the original text projection T_{seq} via element-wise addition:

$$Z_{\text{text}} = Z_{t \rightarrow i} + T_{\text{seq}}, \quad (8)$$

as shown in Equation (8). Similarly, for the image modality, we input the gated text feature $\tilde{T} \in \mathbb{R}^{B \times 1 \times D}$ into the image-to-text MambaFormer encoder:

$$Z_{i \rightarrow t} = \text{MambaFormerEncoder}(\tilde{T}) \in \mathbb{R}^{B \times 1 \times D}, \quad (9)$$

and fuse it with the original image projection I_{seq} by element-wise addition:

$$Z_{\text{img}} = Z_{i \rightarrow t} + I_{\text{seq}}. \quad (10)$$

Cross-Attention: To further improve cross-modal alignment, an additional layer of cross-attention [9] is introduced. First, we let the text query T_{seq} attend to the image features I_{seq} , computing:

$$T_{\text{cross}} = \text{CrossAttn}(Q = T_{\text{seq}}, K = I_{\text{seq}}, V = I_{\text{seq}}) \in \mathbb{R}^{B \times 1 \times D}, \quad (11)$$

which highlights image elements relevant to the text modality. Similarly, for the image modality, we compute:

$$I_{\text{cross}} = \text{CrossAttn}(Q = I_{\text{seq}}, K = T_{\text{seq}}, V = T_{\text{seq}}) \in \mathbb{R}^{B \times 1 \times D}, \quad (12)$$

capturing text elements informative for the image modality. The modality-specific representations are then updated by integrating these cross-attention outputs:

$$Z_{\text{text}}^{\text{final}} = Z_{\text{text}} + T_{\text{cross}}, \quad (13)$$

$$Z_{\text{img}}^{\text{final}} = Z_{\text{img}} + I_{\text{cross}}, \quad (14)$$

as detailed in Equations (13) and (14).

By employing dual-path encoding, we refine modality-specific features using the contextual modeling capacity of MambaFormer-based encoders. The additional cross-attention layers (Equations (11) and (12)) further align the representations by integrating complementary information from each modality. This processing chain improves the overall quality of the extracted features, ensuring effective capture of complementary cues for subsequent fusion.

D. Expert Fusion

TABLE I: Class Distributions Before and After Addressing Class Imbalance for MIMIC and Memotion Datasets

Dataset	Description	Original	Balanced
MIMIC	Non Misogynistic	2497	2497
	Misogynistic	2409	2497
Memotion	not_offensive	2657	2657
	slight	2536	2657
	very_offensive	1424	2657
	hateful_offensive	213	2657

Note: The Memotion dataset mapping is {"not_offensive": 0, "slight": 1, "very_offensive": 2, "hateful_offensive": 3}.

After aligning and refining the modality-specific features through dual-path encoding and additional cross-attention, we fuse the resulting experts into a single unified representation using an advanced expert fusion module.

Concatenation: First, the final text and image representations are concatenated along the feature dimension:

$$C = [Z_{\text{text}}^{\text{final}}; Z_{\text{img}}^{\text{final}}] \in \mathbb{R}^{B \times 2D}, \quad (15)$$

which combines complementary information from both modalities into a joint representation C .

Fusion Network: The concatenated features are then transformed using a feed-forward network with a non-linear activation [9]. The network produces an intermediate fused feature:

$$F = \phi(W_f C + b_f) \in \mathbb{R}^{B \times D}, \quad (16)$$

where $\phi(\cdot)$ (e.g., ReLU) introduces non-linearity. This step synthesizes the information from both text and image modalities.

Gating Weight Computation: Next, we adaptively balance the modality contributions by computing gating weights. The gating network applies a linear transformation followed by a softmax function to C [30]:

$$g = \text{softmax}(W_g C + b_g) \in \mathbb{R}^{B \times 2}, \quad (17)$$

where $g = [g_{\text{text}}, g_{\text{img}}]$ with each component representing the weight for the corresponding modality. The weighted expert sum is then computed as:

$$S = g_{\text{text}} \odot Z_{\text{text}}^{\text{final}} + g_{\text{img}} \odot Z_{\text{img}}^{\text{final}} \in \mathbb{R}^{B \times D}, \quad (18)$$

where \odot denotes element-wise multiplication.

Self-Attention Refinement: To further refine the fused representation, we apply an additional self-attention layer [9]. First, we reshape S into a sequence of length one:

$$S_{\text{seq}} \in \mathbb{R}^{1 \times B \times D}, \quad (19)$$

and then compute:

$$A = \text{MHA}(S_{\text{seq}}, S_{\text{seq}}, S_{\text{seq}}) \in \mathbb{R}^{1 \times B \times D}, \quad (20)$$

after which A is reshaped back to $\mathbb{R}^{B \times D}$.

Final Fusion: The final unified multi-modal representation is obtained by summing the outputs of the fusion network, the weighted expert sum, and the self-attention refinement, followed by layer normalization [31]:

$$E = \text{LayerNorm}(F + S + A) \in \mathbb{R}^{B \times D}. \quad (21)$$

This final representation E encapsulates the complementary and dynamic interactions between the text and image features, preparing it for the classification stage.

Overall, the advanced expert fusion module leverages concatenation, adaptive gating via mixture-of-experts techniques [30], and self-attention to integrate and refine modality-specific features. Equations (15) through (21) illustrate the step-by-step process that ensures the final representation robustly captures the essential information for effective offensive content detection.

TABLE II: Baseline Performance on MIMIC and Memotion Datasets (Accuracy and Macro F1 in %)

Model	MIMIC (%)		Memotion (%)	
	Acc (↑)	F1 (↑)	Acc (↑)	F1 (↑)
mBERT [6]	77.98	77.59	—	—
BERT [6]	—	—	78.60	78.82
DistilBERT [32]	—	—	75.71	75.78
VGG16 [7]	84.58	84.58	76.83	76.78
ResNet50 [33]	84.68	84.56	77.36	77.25
EfficientNetV2 [34]	81.68	81.65	62.14	61.20
XLM-RoBERTa [35]	49.55	43.13	—	—
mBERT-VGG16	85.19	85.16	—	—
mBERT-ResNet50	85.99	85.98	—	—
mBERT-Efficient	83.08	82.90	—	—
RoBERTa + ResNet50	86.29	86.29	—	—
RoBERTa + VGG16	85.09	85.09	—	—
RoBERTa + Efficient	82.28	82.24	—	—
mCLIP [36]	85.79	85.78	82.60	82.66
VisualBERT [37]	<u>86.39</u>	<u>86.39</u>	81.28	81.26
BERT-ResNet50	—	—	82.08	82.00
BERT-Efficient	—	—	79.21	78.94
BERT-VGG16	—	—	81.10	81.00
DistilBERT-ResNet50	—	—	81.28	81.03
DistilBERT-VGG16	—	—	81.14	81.07
DistilBERT-Efficient	—	—	51.98	49.73
Co-AttenDWG	87.19	87.16	84.29	84.26
Improvements	(+0.80↑)	(+0.77↑)	(+1.69↑)	(+1.60↑)

Note: RoBERTa = XLM-RoBERTa [35], Efficient = EfficientNetV2 [34].

TABLE III: Ablation Study and Full Model Performance on Memotion and MIMIC Datasets (Accuracy and Macro F1 in %)

Experiment	MIMIC (%)		Memotion (%)	
	Acc (↑)	F1 (↑)	Acc (↑)	F1 (↑)
No ExpertFusion	83.58	83.56	80.90	80.84
No Co-Attention	85.59	85.57	81.19	81.01
No Cross-Attention	83.58	83.57	79.12	79.26
No MambaFormer	84.98	84.95	81.19	81.31
No Conv in MambaFormer	84.78	84.77	79.49	79.63
Co-AttenDWG	87.19	87.16	84.29	84.26

E. Classification

After obtaining the unified multi-modal representation $E \in \mathbb{R}^{B \times D}$, a linear classifier is applied to map this representation to class logits for C classes. The classifier transforms the multi-modal features into logits, which are then normalized using the softmax function to yield predicted class probabilities. The final predicted class for each sample is determined by selecting the class with the highest probability. The entire model is trained end-to-end using cross-entropy loss, comparing the predicted probabilities with the true class labels. Optimization is performed using the AdamW optimizer with an appropriate learning rate schedule. During training, both the pre-trained encoders (for text and image) and the fusion and classification layers are fine-tuned to learn effective cross-modal interactions that facilitate robust offensive content detection.

IV. EXPERIMENT AND RESULT ANALYSIS

A. Datasets

We evaluate our approach using two publicly available datasets. The first is the SemEval-2020 Memotion Analysis 1.0

TABLE IV: Co-AttenDWG Performance using different backbone models on MIMIC and Memotion Datasets (Accuracy and F1 in %)

Backbone		Datasets			
Text	Image	MIMIC (%)		Memotion (%)	
		Acc	F1	Acc	F1
mBERT	ResNet50	85.29	85.26	–	–
mBERT	VGG16	86.77	86.83	–	–
mBERT	EfficientNetV2	85.28	85.27	–	–
XLM-RoBERTa	ResNet50	87.79	87.83	–	–
XLM-RoBERTa	VGG16	86.17	86.82	–	–
XLM-RoBERTa	EfficientNetV2	82.58	82.86	–	–
BERT	ResNet50	–	–	84.29	84.26
BERT	VGG16	–	–	83.66	83.21
BERT	EfficientNetV2	–	–	83.66	83.21
DistilBERT	ResNet50	–	–	81.81	81.89
DistilBERT	VGG16	–	–	82.09	82.97
DistilBERT	EfficientNetV2	–	–	79.97	80.01

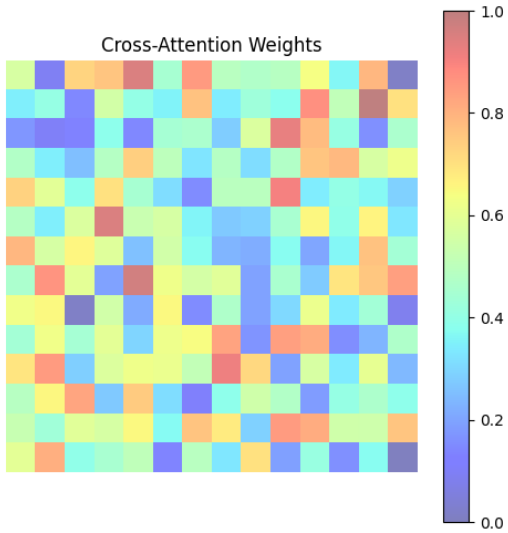
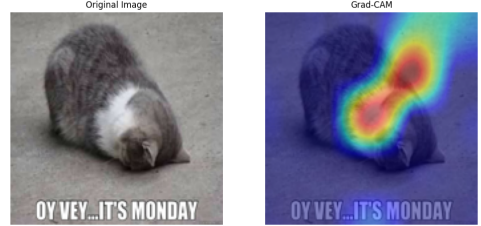


Fig. 3: Cross-attention weight distribution in our Co-AttenDWG architecture. Each cell represents the attention magnitude from a text token to a visual feature. Warmer colors indicate higher attention, and cooler colors indicate lower attention, with the scale ranging from 0 (lowest) to 1 (highest).

dataset [38], which serves as a benchmark for offensive content detection in social media and provides diverse examples of memes along with detailed annotations that capture varying degrees of offensiveness. The second dataset, MIMIC: Misogyny Identification in Multimodal Internet Content in Hindi-English Code-Mixed Language [39], focuses specifically on detecting misogynistic content within multimodal posts characterized by code-mixed language, posing unique challenges for cross-modal understanding. Together, these datasets offer a comprehensive testing ground for our Co-AttenDWG architecture, enabling us to assess its performance in diverse and culturally nuanced contexts. Table I presents dataset statistics.



(a) Original cat meme (left) and Grad-CAM heatmap (right) highlighting salient regions for the classifier.



(b) Original political meme (left) and Grad-CAM heatmap (right). The model focuses on the main subject and text.

Fig. 4: Examples of Grad-CAM visualizations demonstrating which regions of the images the model deems most salient. Figure (a) shows a “cat meme” context, while Figure (b) depicts a political scene. In both cases, the heatmap on the right reveals how the Co-AttenDWG classifier interprets key visual clues.

B. Implementation Details

We implement our model in Python 3.12.1 using PyTorch version 2.0.1 on an NVIDIA RTX 2060 GPU with 16 GB of RAM. We use the AdamW optimizer with a fixed learning rate of 2×10^{-5} and train the model for 20 epochs while employing a learning rate scheduler that dynamically adjusts the rate during training. In our architecture, we set the number of attention heads in the fusion modules to 8 and use 4 heads in the additional self-attention refinement layer. The MambaFormer encoders are configured with a kernel size of 3, a depth of 2 layers, and a dropout rate of 0.1 across all modules. We fine-tune all components, including the pre-trained text encoder (BERT, XLM-RoBERTa) and the image encoder (ResNet50), in an end-to-end manner.

For data preparation, we clean and normalize the input text and images, tokenize the text using the BERT tokenizer, and resize and normalize the images to the required input dimensions. Specifically, for the MIMIC dataset, images are resized to 200×200 pixels. For the SemEval Memotion 1.0 dataset, we use a lower resolution of 160×160 pixels due to resource constraints. We split our datasets from MIMIC and SemEval Memotion 1.0 into 80% for training and 20% for testing and evaluate our model using test accuracy and macro F1-score as our primary metrics. To further enhance performance, we address class imbalance through upsampling [40], ensuring that minority classes are well represented during training. These specific hyperparameter settings, along with

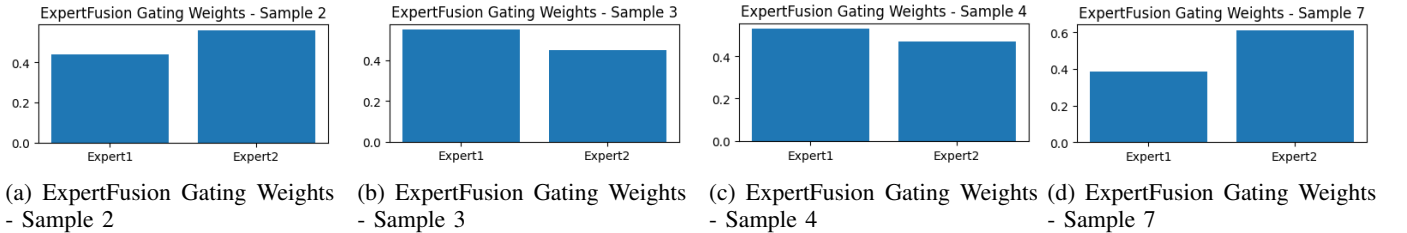
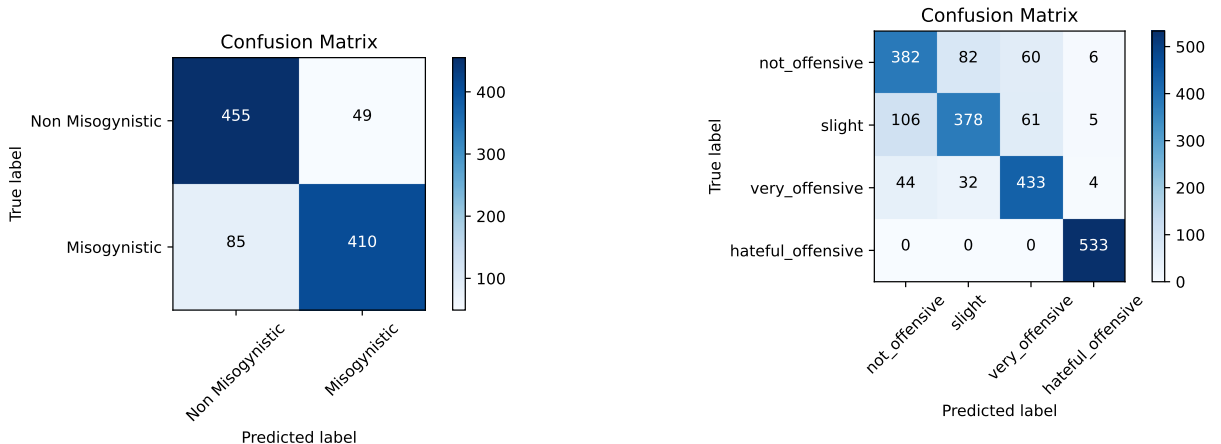


Fig. 5: Bar plots illustrating the gating weights assigned to each expert for different samples in the ExpertFusion module. Each Figure (a, b, c, d) corresponds to a distinct sample, showcasing how the gating mechanism adapts to different inputs.



(a) Confusion matrix for the MIMIC dataset. The true classes are Non Misogynistic (top-left) and Misogynistic (bottom-right).

(b) Confusion matrix for the SemEval Memotion 1.0 dataset, showing not_offensive (top-left), slight, very_offensive, and hateful_offensive classes (bottom-right).

Fig. 6: Confusion matrices for (a) the MIMIC dataset and (b) the Memotion dataset. The diagonal cells represent correct classifications, while off-diagonal cells indicate misclassifications. The color intensity in each cell corresponds to the proportion of samples relative to the total in that true class.

our rigorous data preparation and evaluation protocols, enable our model to effectively learn cross-modal interactions and robustly detect offensive content in multimodal data.

C. Baseline Comparison

Table II presents a comprehensive comparison of baseline model performance on the MIMIC and SemEval Memotion 1.0 datasets. The table reports two key metrics, Test Accuracy and Macro F1 (both expressed as percentages, with higher values indicating better performance), for each model. We compare several unimodal models (for example, mBERT, BERT, and DistilBERT for text and VGG16, ResNet50, EfficientNetV2, and XLM-RoBERTa for image) as well as various multimodal models that combine different text and image backbones in diverse configurations. Notably, our proposed model, Co-AttenDWG, is listed at the bottom of the table to highlight its superior performance. For clarity, the second-best scores in each column are underlined (for instance, VisualBERT and mCLIP achieve the highest results among the alternative configurations in the MIMIC and Memotion settings, respectively). The improvement row indicates the absolute gains of the Co-AttenDWG model over these second-best baselines, showing improvements of +0.80% in MIMIC Accuracy, +0.77% in MIMIC Macro F1, +1.69% in Memotion Accuracy, and +1.60% in Memotion Macro F1. This detailed

comparison emphasizes the robustness of the Co-AttenDWG architecture and demonstrates that integrating enhanced cross-modal interactions and adaptive feature gating leads to significant performance improvements on both datasets.

D. Ablation Study

Table III reports the results of our ablation experiments on the MIMIC and SemEval Memotion 1.0 datasets. In this study, we systematically remove specific components of the proposed Co-AttenDWG architecture to assess their impact on overall performance. The reported metrics are Test Accuracy and Macro F1, both expressed as percentages (with higher values indicating better performance). The first set of experiments involves removing critical modules one at a time. For example, the "No ExpertFusion" experiment excludes the expert fusion module, resulting in a notable performance drop on both datasets. Similarly, when the co-attention mechanism is removed ("No Co-Attention"), the decrease in performance on both MIMIC and Memotion is evident. The "No Cross-Attention" and "No MambaFormer" experiments further illustrate that eliminating the cross-attention layer and the MambaFormer-based encoder modules, respectively, leads to reduced accuracy and Macro F1 scores. The removal of the convolutional operations from the MambaFormer module ("No Conv in MambaFormer") also affects the performance, though



Fig. 7: Case study examples on offensive content detection. The top two Figures are Memotion samples with true labels "not_offensive" (Figure (a)) and "hateful_offensive" (Figure (b)). In Figure (a), mCLIP fails to detect offensive content (indicated by a cross mark), while VisualBERT and Co-AttenDWG correctly classify the sample; in Figure (b), all three models correctly predict the offensive content. The bottom two Figures depict MIMIC samples with the true label "misogyny". In Figure (c), all models produce the correct prediction, whereas in Figure (d) VisualBERT produces an incorrect result (cross mark) while mCLIP and Co-AttenDWG classify the sample correctly.

to a slightly lesser degree. Finally, the full Co-AttenDWG model achieves the best results, demonstrating that every component contributes positively to the overall performance. These results underscore the critical role of each individual module in ensuring effective cross-modal feature integration and alignment.

E. Findings

Table IV summarizes the performance of the proposed Co-AttenDWG architecture when various combinations of text and image backbones are employed on the MIMIC and Memotion datasets. For the MIMIC dataset, only multimodal configurations using text backbones such as mBERT and XLM-RoBERTa paired with image backbones (ResNet50, VGG16, and EfficientNetV2) are evaluated. The results reveal that the combination of XLM-RoBERTa with ResNet50 achieves the highest performance, with an Accuracy of 87.79% and an F1 score of 87.83%. This indicates that a highly expressive text encoder paired with a robust image feature extractor can effectively capture the nuances of the MIMIC dataset. For the Memotion dataset, only configurations involving BERT and DistilBERT are reported. Among these, the BERT paired with ResNet50 configuration produces the best results, yielding an Accuracy of 84.29% and an F1 score of 84.26%. These findings demonstrate that the optimal backbone combination is data-dependent, with different modalities and dataset characteristics favoring distinct model pairings. Overall, the experimental results validate the effectiveness of the Co-AttenDWG architecture in enhancing cross-modal feature integration and emphasize that careful backbone selection is crucial in achieving state-of-the-art performance in multimodal learning tasks.

Figure 3 shows a heatmap of the cross-attention weights in our Co-AttenDWG architecture. Each cell represents the attention strength from a text token to a particular visual feature, with warmer colors indicating higher attention and

cooler colors indicating lower attention. The color scale ranges from 0 (lowest) to 1 (highest), revealing how the model dynamically aligns textual cues with relevant visual regions. Through this visualization, we can observe the degree to which certain words focus on specific parts of the image, offering insight into how the Co-AttenDWG architecture captures cross-modal dependencies and integrates complementary information. These results provide clear evidence that the learned attention distribution corresponds to meaningful semantic regions, reinforcing the effectiveness of the co-attention module. Furthermore, the heatmap demonstrates that our approach can flexibly adapt to varied input content, thereby enhancing interpretability and overall performance.

Figure 4 illustrates Grad-CAM visualizations that reveal which regions of each image the classifier deems most salient. In Figure (4a), the "cat meme" context is shown on the left, while the corresponding Grad-CAM heatmap on the right highlights areas where the model concentrates its attention. In Figure (4b), the original political meme appears on the left, and the heatmap on the right indicates the focus on both the main subject and any prominent text. These examples illustrate how the Co-AttenDWG classifier interprets visual features and aligns them with relevant textual cues to make its predictions. Furthermore, the Grad-CAM outputs provide a clear, interpretable validation of the model's focus areas, confirming that salient image regions such as key objects and texts directly contribute to the classification outcome. This insight not only demonstrates the model's effectiveness in capturing meaningful visual patterns but also enhances our understanding of the underlying decision-making process.

Figure 5 presents four bar plots that show the gating weights assigned to each expert for different samples in the ExpertFusion module. In Figure (5a), the gating mechanism assigns a relatively high weight to expert 1, indicating that for this sample the features extracted by expert 1 are the most important for the prediction, while the contributions

from experts 2 and 3 are substantially lower. In [Figure \(5b\)](#), the plot displays a more even distribution of weights, with expert 2 receiving a slightly higher value than the others, which suggests that this sample benefits from a balanced combination of information from multiple experts instead of a single dominant source. In [Figure \(5c\)](#), the plot clearly shows that expert 3 receives a much higher weight compared to the other experts, indicating that for that particular sample the key discriminative features are predominantly captured by expert 3. Finally, [Figure \(5d\)](#) demonstrates another scenario in which one expert is strongly favored by the gating mechanism, with expert 1 again receiving the highest weight. Overall, these Figures provide clear insight into how the ExpertFusion module dynamically adjusts the importance of each expert in response to different input characteristics, thereby enhancing the effectiveness of the overall multi-modal representation.

F. Error Analysis

[Figure 6](#) presents the confusion matrices for both the MIMIC and Memotion datasets, providing a detailed view of the classification performance. In [Figure \(6a\)](#) for the MIMIC dataset, the majority of samples are correctly classified as either Non Misogynistic or Misogynistic. However, a number of misogynistic samples are incorrectly predicted as non-misogynistic, which indicates that the model sometimes struggles with distinguishing subtle cues between these classes. These errors may stem from ambiguous visual or textual content that does not distinctly signal misogyny. In [Figure \(6b\)](#) for the Memotion dataset, we observe that misclassifications mainly occur among the offensive classes with close intensity levels, such as between "slight" and "very_offensive." This suggests that there is considerable overlap in the feature space of these classes, which can be attributed to nuanced differences in language and image contexts. Overall, both Figures highlight that while the model performs well on overall classification, there remain challenges in precisely delineating fine-grained differences between closely related offensive categories. Addressing these issues may require enhanced feature extraction methods and improved annotation consistency.

[Figure 7](#) presents four representative examples that illustrate the performance of the Co-AttenDWG architecture in detecting offensive content from memes, demonstrating its effectiveness in comparison with mCLIP and VisualBERT. In [Figure \(7a\)](#), a Memotion sample with a true label of "not_offensive" is shown; here VisualBERT and Co-AttenDWG produce the correct outcome, while mCLIP fails to correctly classify the sample as non-offensive. [Figure \(7b\)](#) features another Memotion sample, with the true label "hateful_offensive," where all three models yield accurate predictions, confirming the robust performance of the models under challenging conditions. Moving to the MIMIC dataset, [Figure \(7c\)](#) illustrates a sample with a true label of "misogyny," and all models—mCLIP, VisualBERT, and Co-AttenDWG—successfully classify the sample, indicating consistent performance when detecting misogynistic content. In [Figure \(7d\)](#), another MIMIC sample labeled "misogyny" is presented; while mCLIP and

Co-AttenDWG correctly identify the offensive content, VisualBERT misclassifies the sample, highlighting subtle differences in model behavior. Overall, this figure provides detailed insight into the decision-making process of the examined architectures, revealing that the Co-AttenDWG model maintains high accuracy in both Memotion and MIMIC scenarios by effectively integrating multimodal cues and adapting to the unique characteristics of each input.

V. CONCLUSIONS

In this work, we introduced the multi-modal Co-AttenDWG architecture, which leverages cross-modal co-attention, dimension-wise gating, dual-path encoding, and advanced expert fusion to dynamically integrate text and image features. Our extensive experiments on the MIMIC and SemEval Memotion 1.0 datasets demonstrate that our approach effectively enhances cross-modal feature integration, leading to significant improvements in classification accuracy and macro F1 scores. While our results validate the benefits of adaptive fusion in multi-modal learning, we acknowledge several limitations. First, the performance of the model is sensitive to the choice of backbone models, suggesting that optimal performance may require dataset-specific adjustments. Second, the computational overhead introduced by multiple attention and gating mechanisms remains a concern for real-time applications. Future work will focus on reducing model complexity and exploring more efficient gating strategies, as well as extending our approach to additional tasks such as retrieval and scene understanding. We also plan to investigate the integration of external knowledge sources to further improve the interpretability and robustness of the system. Overall, our findings underscore the potential of adaptive fusion techniques in multi-modal learning and open promising directions for future research.

REFERENCES

- [1] T. Baltrušaitis, C. Ahuja, and L.-P. Morency, "Multimodal machine learning: A survey and taxonomy," *IEEE transactions on pattern analysis and machine intelligence*, vol. 41, no. 2, pp. 423–443, 2018.
- [2] J. Ngiam, A. Khosla, M. Kim, J. Nam, H. Lee, and A. Y. Ng, "Multimodal deep learning," in *Proceedings of the 28th International Conference on Machine Learning (ICML)*, 2011, pp. 689–696.
- [3] A. Singh, D. Sharma, and V. K. Singh, "Emogif: A multimodal approach to detect emotional support in animated gifs," *IEEE Transactions on Computational Social Systems*, 2025.
- [4] K. Xu, J. Ba, R. Kiros, K. Cho, A. Courville, R. Salakhutdinov, R. Zemel, and Y. Bengio, "Show, attend and tell: Neural image caption generation with visual attention," in *Proceedings of the 32nd International Conference on Machine Learning (ICML)*, 2015, pp. 2048–2057.
- [5] G. V. Singh, A. Verma, A. Ekbal *et al.*, "Multiseao-mix: A multimodal multitask framework for sentiment, emotion, support, and offensive analysis in code-mixed setting," *IEEE Transactions on Computational Social Systems*, 2024.
- [6] J. Devlin, M.-W. Chang, K. Lee, and K. Toutanova, "Bert: Pre-training of deep bidirectional transformers for language understanding," in *Proceedings of the 2019 conference of the North American chapter of the association for computational linguistics: human language technologies, volume 1 (long and short papers)*, 2019, pp. 4171–4186.
- [7] K. Simonyan and A. Zisserman, "Very deep convolutional networks for large-scale image recognition," *arXiv preprint arXiv:1409.1556*, 2014.
- [8] A. Krizhevsky, I. Sutskever, and G. E. Hinton, "Imagenet classification with deep convolutional neural networks," in *Advances in Neural Information Processing Systems (NIPS)*, 2012, pp. 1097–1105.

[9] A. Vaswani, N. Shazeer, N. Parmar, J. Uszkoreit, L. Jones, A. N. Gomez, Ł. Kaiser, and I. Polosukhin, "Attention is all you need," *Advances in neural information processing systems*, vol. 30, 2017.

[10] A. Rana and S. Jha, "Emotion based hate speech detection using multimodal learning," *arXiv preprint arXiv:2202.06218*, 2022.

[11] A. Birhane, V. Prabhu, and E. Kahembwe, "Multimodal datasets: misogyny, pornography, and malignant stereotypes," *arXiv preprint arXiv:2110.01963*, 2021.

[12] S. Suryawanshi, B. Chakravarthi, M. Arcan, and P. Buitelaar, "Multimodal meme dataset (multioff) for identifying offensive content in image and text," in *Proceedings of the Second Workshop on Trolling, Aggression and Cyberbullying*, 2020, pp. 32–41.

[13] J. Paul, S. Mallick, A. Mitra, A. Roy, and J. Sil, "Multi-modal twitter data analysis for identifying offensive posts using a deep cross attention based transformer framework," *ACM Transactions on Knowledge Discovery from Data*, 2025.

[14] J. Mu, W. Wang, W. Liu, T. Yan, and G. Wang, "Multimodal large language model with lora fine-tuning for multimodal sentiment analysis," *ACM Transactions on Intelligent Systems and Technology*, 2024.

[15] F. Huang, X. Zhang, Z. Zhao, J. Xu, and Z. Li, "Image–text sentiment analysis via deep multimodal attentional fusion," *Knowledge-Based Systems*, vol. 167, pp. 26–37, 2019.

[16] T. S. Ataei, K. Darvishi, S. Javdan, A. Pourdabiri, B. Minaei-Bidgoli, and M. T. Pilehvar, "Pars-off: a benchmark for offensive language detection on farsi social media," *IEEE Transactions on Affective Computing*, vol. 14, no. 4, pp. 2787–2795, 2022.

[17] Y. Zheng, J. Gong, Y. Wen, and P. Zhang, "Djmf: A discriminative joint multi-task framework for multimodal sentiment analysis based on intra- and inter-task dynamics," *Expert Systems with Applications*, vol. 242, p. 122728, 2024.

[18] D. Chen, W. Su, P. Wu, and B. Hua, "Joint multimodal sentiment analysis based on information relevance," *Information Processing & Management*, vol. 60, no. 2, p. 103193, 2023.

[19] F. Abdullakutty and U. Naseem, "Decoding memes: a comprehensive analysis of late and early fusion models for explainable meme analysis," in *Companion Proceedings of the ACM Web Conference 2024*, May 2024, pp. 1681–1689.

[20] L. Zhu, Z. Zhu, C. Zhang, Y. Xu, and X. Kong, "Multimodal sentiment analysis based on fusion methods: A survey," *Information Fusion*, vol. 95, pp. 306–325, 2023.

[21] A. Gandhi, K. Adhvaryu, S. Poria, E. Cambria, and A. Hussain, "Multimodal sentiment analysis: A systematic review of history, datasets, multimodal fusion methods, applications, challenges and future directions," *Information Fusion*, vol. 91, pp. 424–444, 2023.

[22] O. Adel, K. Fathalla, and A. Abo ElFarag, "Mm-emor: multi-modal emotion recognition of social media using concatenated deep learning networks," *Big Data and Cognitive Computing*, vol. 7, no. 4, p. 164, 2023.

[23] Z. Zhou, H. Feng, B. Qiao, G. Wu, and D. Han, "Syntax-aware hybrid prompt model for few-shot multi-modal sentiment analysis," *arXiv preprint arXiv:2306.01312*, 2023.

[24] A. A. Khan, M. H. Iqbal, S. Nisar, A. Ahmad, and W. Iqbal, "Offensive language detection for low resource language using deep sequence model," *IEEE Transactions on Computational Social Systems*, 2023.

[25] J. Mao, H. Shi, and X. Li, "Research on multimodal hate speech detection based on self-attention mechanism feature fusion," *The Journal of Supercomputing*, vol. 81, no. 1, p. 28, 2025.

[26] H. Li, Y. Lu, and H. Zhu, "Multi-modal sentiment analysis based on image and text fusion using a cross-attention mechanism," *Electronics*, vol. 13, no. 11, p. 2069, 2024.

[27] L. Hebert, G. Sahu, Y. Guo, N. Sreenivas, L. Golab, and R. Cohen, "Multi-modal discussion transformer: Integrating text, images and graph transformers to detect hate speech on social media," in *Proceedings of the AAAI Conference on Artificial Intelligence*, vol. 38, no. 20, March 2024, pp. 22096–22104.

[28] B. Liang, L. Gui, Y. He, E. Cambria, and R. Xu, "Fusion and discrimination: A multimodal graph contrastive learning framework for multimodal sarcasm detection," *IEEE Transactions on Affective Computing*, 2024.

[29] J. Hu, L. Shen, and G. Sun, "Squeeze-and-excitation networks," in *Proceedings of the IEEE Conference on Computer Vision and Pattern Recognition (CVPR)*, 2018, pp. 7132–7141.

[30] N. Shazeer, A. Mirhoseini, K. Maziarz, A. Davis, Q. V. Le, and G. Hinton, "Outrageously large neural networks: The sparsely-gated mixture-of-experts layer," in *International Conference on Learning Representations (ICLR)*, 2017.

[31] J. L. Ba, J. R. Kiros, and G. E. Hinton, "Layer normalization," *arXiv preprint arXiv:1607.06450*, 2016.

[32] V. Sanh, L. Debut, J. Chaumond, and T. Wolf, "Distilbert, a distilled version of bert: smaller, faster, cheaper and lighter," *arXiv preprint arXiv:1910.01108*, 2019.

[33] K. He, X. Zhang, S. Ren, and J. Sun, "Deep residual learning for image recognition," in *CVPR*, 2016.

[34] M. Tan and Q. V. Le, "Efficientnetv2: Smaller models and faster training," in *ICML*, 2021.

[35] A. Conneau, K. Khandelwal, N. Goyal, V. Chaudhary, G. Wenzek, F. Guzmán, and V. Stoyanov, "Unsupervised cross-lingual representation learning at scale," *NAACL-HLT*, 2019.

[36] A. Radford, J. W. Kim, C. Hallacy, A. Ramesh, G. Goh, S. Agarwal, G. Sastry, A. Askell, P. Mishkin, J. Clark, and I. Sutskever, "Learning transferable visual models from natural language supervision," *arXiv preprint arXiv:2103.00020*, 2021.

[37] L.-h. Li, M. Yatskar, K.-W. Chang, J. Lin, and E. Hovy, "Visualbert: A simple and performant baseline for vision and language," in *NAACL-HLT*, 2019.

[38] C. Sharma, W. Paka, D. B. Scott, A. Das, S. Poria, T. Chakraborty, and B. Gambäck, "Task report: Memotion analysis 1.0@ semeval 2020: The visuo-lingual metaphor," in *Proceedings of the 14th International Workshop on Semantic Evaluation (SemEval-2020)*. Association for Computational Linguistics, 2020, pp. 0–0.

[39] A. Singh, D. Sharma, and V. K. Singh, "Mimic: misogyny identification in multimodal internet content in hindi-english code-mixed language," *ACM Transactions on Asian and Low-Resource Language Information Processing*, 2024.

[40] M. M. Hossain, M. S. Hossain, M. S. Hossain, M. Mridha, M. Safran, and S. Alfarhood, "Transnet: Deep attentional hybrid transformer for arabic posts classification," *IEEE Access*, 2024.